Available online at www.sciencedirect.com

ScienceDirect

Journal of Catalysis 252 (2007) 171–177

JOURNAL OF CATALYSIS

www.elsevier.com/locate/jcat

# CO adsorption energy on planar Au/$TiO_2$ model catalysts under catalytically relevant conditions

T. Diemant, H. Hartmann, J. Bansmann, R.J. Behm [*]

*Institute of Surface Chemistry and Catalysis, Ulm University, D-89069 Ulm, Germany*

Received 20 June 2007; revised 25 September 2007; accepted 30 September 2007

## Abstract

The adsorption of CO on planar Au/$TiO_2$ model catalysts was studied by polarization-modulation infrared reflection–absorption spectroscopy (PM-IRAS) under catalytically relevant pressure (10–50 mbar) and temperature (30–120 °C) conditions, both in pure CO and in CO/$O_2$ reaction gas mixtures. The adsorption energy of CO on the Au particles was determined by a quantitative analysis of the temperature dependence of the CO absorption intensity in adsorption isobars. The data reveal considerable effects of the Au particle size when pure CO is used; the initial adsorption energy decreases from 74 kJ $mol^{-1}$ (2 nm mean Au particle diameter) to 62 kJ $mol^{-1}$ (4 nm). For CO/$O_2$ gas mixtures, the initial CO adsorption energy is, irrespective of the Au particle size, constant at 63 kJ $mol^{-1}$ (i.e., the CO adsorption energy is reduced for smaller Au particles), but this effect vanishes for larger Au particles.

*Keywords:* IR absorption–reflection spectroscopy; Adsorption energy; Coadsorption; Model catalyst; Gold; Titanium oxide; Carbon monoxide; Oxygen

## 1. Introduction

Finely dispersed Au particles of <5 nm diameter supported on metal oxides show surprisingly high activity in a number of catalytic reactions, the most prominent one being the low-temperature CO oxidation [1–3]. Despite intense research efforts in recent, some basic aspects of the underlying reaction mechanism remain unresolved. Most important for the mechanistic understanding of the CO oxidation reaction, the activation of molecular oxygen and, closely related, the nature of the active site remain unclear for these catalysts, and it is questionable whether a single reaction pathway is sufficient to describe the reaction under different reaction conditions [4] and on Au catalysts supported by different oxides [5]. On the other hand, considering the weak interaction between bulk Au and CO [6–14], the adsorption of CO on these catalysts is highly important as well and, through the steady-state $CO_{ad}$ coverage, will affect the reaction rate.

IR spectroscopic studies on realistic Au/$TiO_2$ catalysts revealed that CO adsorbs under reaction conditions in a linear configuration on the Au nanoparticles [15,16]. From the position of the CO vibration, which is normally detected at around 2100 $cm^{-1}$, it may be concluded that the Au nanoparticles are in a metallic state [17]. Similar results also were obtained on well-defined model catalysts [18,19], where, based on the preparation procedure, the presence of ionic Au species can be excluded. Recently, we demonstrated that for Au/$TiO_2$ model catalysts, interaction with CO at higher pressure (>20 mbar) leads to the emergence of a new IR signal at around 2060 $cm^{-1}$ [20]. We attributed this signal to the formation of negatively charged $Au^{\delta-}$ particles generated through reduction of the substrate, by reaction of CO with surface oxygen. We observed a similar effect of CO on dispersed powder Au/$TiO_2$ catalysts at even lower CO pressure (1 mbar), leading in this case to the complete disappearance of the initial signal at 2100 $cm^{-1}$ [21].

The adsorption energy of CO on these catalysts has been the topic of a number of studies on both realistic catalysts [22] and planar model systems [18,19,23,24]. Based on a quantitative analysis of their IR results, Derrouiche et al. determined that the adsorption energy for CO on a Au/$TiO_2$ powder catalyst decreased with increasing CO coverage, from 74 to

---

[*] Corresponding author.
*E-mail address:* juergen.behm@uni-ulm.de (R.J. Behm).

0021-9517/$ – see front matter © 2007 Elsevier Inc. All rights reserved.
doi:10.1016/j.jcat.2007.09.024

47 kJ mol$^{-1}$ [22]. Studies on planar Au/TiO$_2$ model catalysts revealed that the CO adsorption energy also depends on the Au particle size [18,19]. For smaller Au particles, an initial CO adsorption energy of 76 kJ mol$^{-1}$ was reported (adsorption energy in the limits of small CO$_{ad}$ coverages), in agreement with the results for powder catalysts. For samples with larger Au particle diameters, the initial CO adsorption energy decreased significantly [18], reaching values of around 50–60 kJ mol$^{-1}$, which are typical for CO adsorption on smooth Au surfaces [6–14], indicating that CO adsorption on the Au particles of the model catalysts converges to a bulk-like character with increasing Au particle size. So far, however, IR spectroscopic studies of CO adsorption on model catalyst or single-crystal samples have been performed under ultra-high-vacuum (UHV) conditions at cryogenic temperatures only, leaving unanswered the pertinent question of whether the results from UHV studies can be extrapolated through the “pressure gap” and transferred to CO adsorption under reaction conditions at elevated pressures in the millibar regime and in the typical temperature range of room temperature to 100 °C.

Using different nominal Au coverages, we studied the influence of the Au particle size on the CO adsorption energy under the above reaction conditions. Possible effects caused by the presence of oxygen as second component in the CO oxidation reaction have not been investigated to date. For CO adsorption on various metal surfaces, it is well known that coadsorption of oxygen modifies the adsorption properties of CO considerably (for, e.g., CO/O coadsorption on Ru(0001) [25]), and similar effects also might occur on Au substrates. These questions are the topic of this paper, where we report results of an in situ IR spectroscopy study on the interaction of CO with a well-defined planar Au/TiO$_2$ model catalyst under temperature and pressure conditions relevant for catalytic reaction studies in both the presence and absence of O$_2$ in the gas phase. CO adsorption energies were derived from the IR intensities using a procedure described first by Bianchi and coworkers [26], which we describe in more detail below. Preliminary IR results obtained at room temperature were presented previously [27].

## 2. Experimental

The experiments were performed in a UHV system with facilities for surface preparation and characterization with an attached high-pressure cell. The design and function of the high-pressure cell has been described in detail previously [28]. Fully oxidized, smooth titania films were prepared by deposition of Ti onto a Ru(0001) substrate in an O$_2$ atmosphere and subsequent annealing steps in O$_2$ (more information in Ref. [19]). These TiO$_2$ films had a thickness of around 10 monolayer equivalents (MLEs), with 1 MLE defined as the amount needed to cover the Ru(0001) single crystal with a closed TiO$_x$ layer [29]. Subsequently, Au was deposited at room temperature on the titania films (deposition rate: 0.04 monolayers (ML) min$^{-1}$). The Au coverage is given with respect to the atom density of the underlying Ru(0001) substrate of $1.6 \times 10^{15}$ Au atoms cm$^{-2}$ as 1 ML.

For the high-pressure IR measurements, the samples were transferred from the UHV section to the high-pressure cell. Before the IR measurements, the samples were first treated in 50 mbar of a CO/O$_2$ gas mixture (2:1) for 30 min at 130 °C to ensure that the Au particles of the model catalyst remained stable throughout the experiment. The IR measurements were performed with a Bruker Tensor 27 spectrometer, using polarization-modulation (PM) techniques to remove the gas-phase CO contribution, which affects the IR measurements at higher pressure. The IR spectra displayed here were acquired by co-addition of 1024 scans with a spectral resolution of 4 cm$^{-1}$.

## 3. Results and discussion

To study the influence of the Au particle size, we used samples with different nominal Au coverages for the IR measurements. Previous STM measurements with identically prepared samples had demonstrated that the deposited Au particles have a rather flat morphology [19,30]. The height of the particles increased from around two to six atomic layers in the Au coverage range covered by this study, from 0.15 to 1.6 ML. At the same time, the mean lateral diameter of the Au particles increased from 2 to 4 nm. A sequence of IR spectra collected in a CO atmosphere of 10 mbar on a sample with 0.21 ML Au at increasing temperatures from 30 to 120 °C is displayed in Fig. 1a. The characteristic feature at 30 °C is an IR band at 2108 cm$^{-1}$, which, following previous assignments [31], is attributed to linearly adsorbed CO on the Au particles. The intensity of the IR peak decreased steadily with increasing temperature, pointing to a reduction of the CO coverage on the Au particles due to increasing desorption. Concurrently, the peak position shifted to slightly higher wave numbers, arriving at 2112 cm$^{-1}$ at 120 °C. After that, the temperature was stepped back to 30 °C to check for possible changes in the frequency or intensity of the peak during the isobaric measurement (Fig. 1a, lowest spectrum), which would indicate irreversible changes of the catalyst such as particle sintering or the pickup of surface contaminations during the IR experiment. Based on the identical appearance of the spectra, such changes can be excluded. In addition to this characteristic CO feature, no other absorption bands were detected [15,22,32].

Fig. 1b displays the development of the CO$_{ad}$ coverage with increasing temperature. It was derived from the integrated CO$_{ad}$ signal intensity, assuming that in the absence of different adsorption sites and for small interactions between adsorbed CO molecules, the cross-section is independent of the CO$_{ad}$ coverage, and thus IR intensity and CO$_{ad}$ coverage are linearly related. The saturation coverage was determined from higher pressure (50–100 mbar) IR measurements in a CO/O$_2$ (2:1) gas mixture. This calibration measurement had to be performed in a CO-rich CO/O$_2$ mixture rather than in pure CO, because at elevated CO pressures ($\geqslant$20 mbar), the interaction of pure CO with the catalyst leads to a modification of the model catalyst surface due to a partial reduction of the TiO$_2$ support and concomitant changes of the Au particle shape [20].

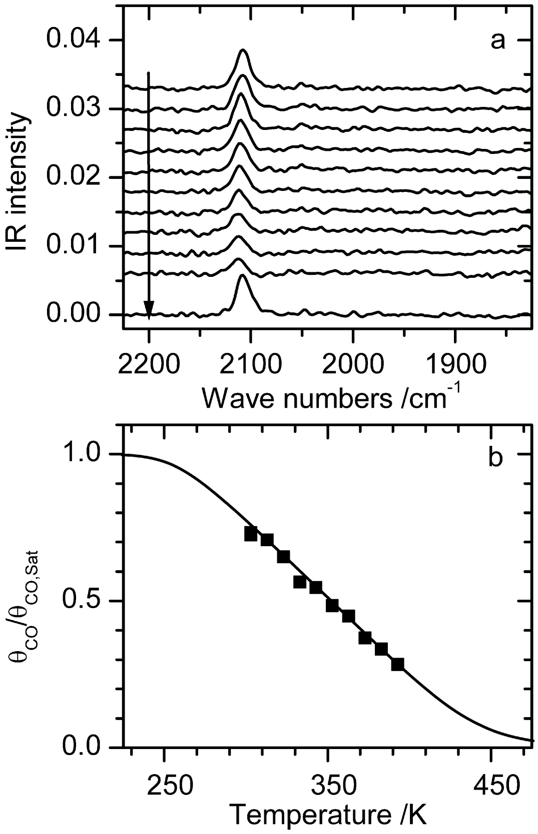

Fig. 1. (a) IR spectra recorded on a Au/TiO$_2$ model catalyst with a nominal Au coverage of 0.21 ML in 10 mbar CO at different temperatures. The spectra are arranged following the course of the experiment (arrow from top to bottom): IR spectra with increasing temperature from 30 to 120 °C (steps of 10 °C), final measurement at 30 °C again. (b) Relative CO coverage on the Au particles as a function of the sample temperature (squares) and calculated adsorption isobar (full line).

For the quantitative analysis of the IR measurements, we used a method developed by Bianchi and coworkers for the study of the adsorption of CO on different metal/metal oxide powder catalysts [26]. This evaluation is based on the assumption of a linear decrease of the adsorption energy of CO with increasing CO$_{ad}$ coverage. In that case, the evolution of the CO$_{ad}$ coverage with decreasing temperature can be described by the following expression [26,33,34]:

$$\theta_{CO} = \frac{RT}{E_0 - E_1} \ln\left(\frac{1 + \lambda_0 p_{CO}}{1 + \lambda_1 p_{CO}}\right), \tag{1}$$

where $E_0$ and $E_1$ represent the CO adsorption energy at very small coverage ($E_0$) and at saturation coverage ($E_1$), respectively. It should be noted that the state corresponding to $E_0$ is always populated in the experiments. Therefore, the value of $E_0$ must be high enough to allow the population of this state under the respective equilibrium conditions, whereas the state corresponding to $E_1$ is not necessarily populated. In fact, for many of the present measurements, the highest CO$_{ad}$ coverage obtained is below saturation coverage. In analogy, $\lambda_0$ and $\lambda_1$ are the adsorption coefficients at minimum ($\lambda_0$) and maximum ($\lambda_1$) CO$_{ad}$ coverages that can be derived using statistical thermodynamics, assuming localized and nonactivated CO adsorption and also neglecting changes of the internal partition function for adsorbed and free CO molecules [26]:

$$\lambda_0 = \left(\frac{h}{\sqrt{2\pi m_{CO} k_B T}}\right)^3 \frac{1}{k_B T} \exp\left(\frac{E_0}{RT}\right), \tag{2}$$

$$\lambda_1 = \left(\frac{h}{\sqrt{2\pi m_{CO} k_B T}}\right)^3 \frac{1}{k_B T} \exp\left(\frac{E_1}{RT}\right), \tag{3}$$

where $h$ is Planck's constant, $k_B$ is Boltzmann's constant, $m_{CO}$ is the mass of a CO molecule, and $E_0$ and $E_1$ represent the CO adsorption energy at minimum and maximum coverage, respectively.

Based on these relations, the development of the CO$_{ad}$ coverage with increasing temperature can be modeled by a calculated adsorption isobar. Within this model, the only free parameters are the adsorption energies at minimum and maximum CO$_{ad}$ coverage, respectively. Bianchi and coworkers applied this method already for the study of CO adsorption on dispersed Au/TiO$_2$ powder catalysts [22] and a number of other supported catalysts with different metal particles, such as Pt [34], Pd [35,36], Rh [37], and Cu [38]. In comparison to an isosteric analysis, the most commonly used method for the analysis of IR experiments (for Au samples, see, e.g., [10,18,39]), the procedure described above is considerably less time-consuming and thus less susceptible to surface contamination.

Equation (1) was used to model the experimental isobaric data (points in Fig. 1b) of the IR experiment with the Au/TiO$_2$ model catalyst with 0.21 ML Au. The best agreement to the experimental isobar is obtained for values of the maximum ($E_0$) and minimum ($E_1$) CO adsorption energy of 74 and 40 kJ mol$^{-1}$, respectively. We tested the error margin of the fitting procedure by varying these two parameters, which resulted in an error of at most $\pm 2$ kJ mol$^{-1}$. We also tested the effect of a nonlinear decay of the adsorption energy with coverage. Based on these tests, significant deviations from a linear decrease of the adsorption energy with CO$_{ad}$ coverage can be ruled out, because they would cause sizable modifications in the shape of the isobars. This conclusion is also supported by the results of a full isosteric analysis of the CO adsorption behavior on a sample with 0.9 ML Au (using 50 mbar of a CO/O$_2$ gas mixture [2:1]), which confirmed an almost linear decrease in adsorption energy with a slightly steeper slope at the lowest CO$_{ad}$ coverage.

The resulting values of $E_0$ and $E_1$ are in excellent agreement with the results of a similar analysis by Derrouiche et al. [22] for the CO adsorption on Au/TiO$_2$ powder catalysts, which gave a decrease of the CO adsorption energy from 74 to 47 kJ mol$^{-1}$ with increasing CO coverage. Furthermore, the initial adsorption energy, $E_0$, also agrees well with the results of a study by Meier et al. [18] who investigated the CO adsorption on planar Au/TiO$_2$ model catalysts under UHV conditions applying an isosteric analysis and obtained an initial adsorption energy of 76 kJ mol$^{-1}$ for a model catalyst with 0.25 ML Au.

Similar type IR measurements as for the Au/TiO$_2$ model catalyst with 0.21 ML Au were also performed on model catalysts with nominal Au coverages of 0.9 and 1.6 ML, respectively. For the sample with 0.9 ML Au, the typical height of the particles was between four and five atomic layers, while the mean

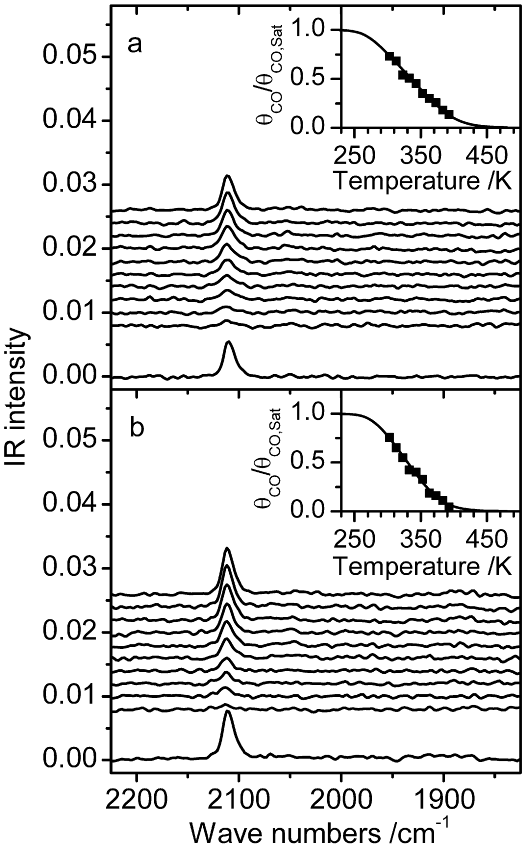

Fig. 2. IR spectra recorded in 10 mbar CO on Au/TiO$_2$ model catalysts with different nominal Au coverages at varying temperatures: (a) 0.9 and (b) 1.6 ML. The insets show the evolution of the relative CO$_{ad}$ coverage on the model catalysts with temperature (squares) and the calculated adsorption isobars (full line).

particle diameter was 3 nm. At 1.6 ML Au, the height was around six layers, and the mean particle diameter was 4 nm [30]. The results of these IR measurements are displayed in Fig. 2. For these two Au coverages, the IR spectra also show the band from linearly adsorbed CO at around 2110 cm$^{-1}$. The evolution of the relative CO$_{ad}$ coverages with increasing temperature is presented in the insets to the corresponding IR spectra of the two samples. Again, the experimental isobar was modeled using Eq. (1). For the 0.9 ML Au sample, the CO adsorption energy started at 66 kJ mol$^{-1}$ and decreased to 42 kJ mol$^{-1}$ with increasing CO coverage; for the 1.6 ML sample, the CO adsorption energy varied from 62 to 44 kJ mol$^{-1}$. It should be noted that CO$_{ad}$ saturation coverages were not reached under the present conditions, and that the extrapolation of the data and hence the value of $E_1$ had a larger error margin than $E_0$. The results of these experiments, summarized in Table 1, show a marked decrease in the initial CO adsorption energy, $E_0$, with increasing Au particle size, from 74 kJ mol$^{-1}$ for the smallest Au coverage to 62 kJ mol$^{-1}$ for the highest Au coverage. The decrease in CO adsorption energy with particle size fully agrees with results of previous studies on the CO adsorption on Au/TiO$_2$ model catalysts performed under UHV conditions [18], and also the absolute values are in good agreement, at least for the lower CO$_{ad}$ coverages [19]. The decrease in CO adsorption energy was explained by a change of the chemical properties of the Au particles with increasing particle thickness, from highly stabilized CO adsorption on monolayer Au islands to weaker adsorption on thicker particles, approaching a bulk-like adsorption behavior with increasing particle size [40,41]. In another explanation, this development was ascribed to a reduced number of undercoordinated sites with special binding properties on the Au particles with increasing particle size [42,43], or a combination of both effects.

Table 1
CO adsorption energies for adsorption on the Au particles of Au/TiO$_2$ model catalysts in a CO atmosphere

| $\theta_{Au}$ (ML) | $p_{CO}$ (mbar) | $E_0$ (kJ mol$^{-1}$) | $E_1$ (kJ mol$^{-1}$) |
|---|---|---|---|
| 0.21 | 10 | 74 | 40 |
| 0.9 | 10 | 66 | 42 |
| 1.6 | 10 | 62 | 44 |

Similar measurements, with samples of nominal Au coverages of 0.15, 0.24, 0.9, and 1.5 ML, were performed in CO/O$_2$ gas mixtures ($p_{CO}$:$p_{O_2}$ = 2:1) instead of pure CO to simulate the situation in a reaction gas mixture. The results of these IR measurements are displayed in Fig. 3. For all Au coverages, the IR spectra show an identical general behavior. They are dominated by a single band, which at 30 °C is situated between 2110 and 2112 cm$^{-1}$. With increasing temperature and thus decreasing CO$_{ad}$ coverage, it shifts to slightly higher wave numbers. Similar to the experiments with pure CO, no other peaks are detected besides this band, excluding the formation of measurable amounts of byproducts of the CO oxidation reaction such as carbonate, which are commonly observed on dispersed Au/TiO$_2$ catalysts (e.g., [16,32]).

The insets of Fig. 3 show again the development of the CO coverage on the Au/TiO$_2$ samples with increasing temperature. In the inset of Fig. 3c, we added results of a similar IR experiment with a reduced gas pressure of 10 mbar (identical composition). When working with reactive CO/O$_2$ gas mixtures, it is important to exclude the possibility that the adsorption–desorption equilibrium, which determines the CO$_{ad}$ steady-state coverage, is significantly altered by the simultaneous CO oxidation reaction. Using a turnover frequency for CO oxidation of 0.35 s$^{-1}$, which had been determined in parallel kinetic measurements at 100 °C and 50 mbar [44], a preexponential factor for desorption of $10^{13}$ s$^{-1}$ and an activation energy for desorption of 65 kJ mol$^{-1}$, the desorption rate was more than 3 orders of magnitude higher than the reaction rate. Therefore, such effects can be ruled out.

The results of the quantitative analysis of the IR spectra recorded in the CO/O$_2$ gas mixture are summarized in Table 2. In these measurements, the initial adsorption energy, $E_0$, remained constant at 63 kJ mol$^{-1}$ for all Au coverages studied. The minimal adsorption energy, $E_1$, decreased slightly with increasing Au coverage from 53 (0.15 ML Au) to 48 kJ mol$^{-1}$ (1.5 ML Au) at 50 mbar total pressure, i.e., similar to the initial adsorption energy $E_0$, the particle size effects were small. Due to the higher CO partial pressures, CO$_{ad}$ coverages of or close to saturation were reached in these experiments. Comparison with the results obtained in a pure CO atmosphere shows that

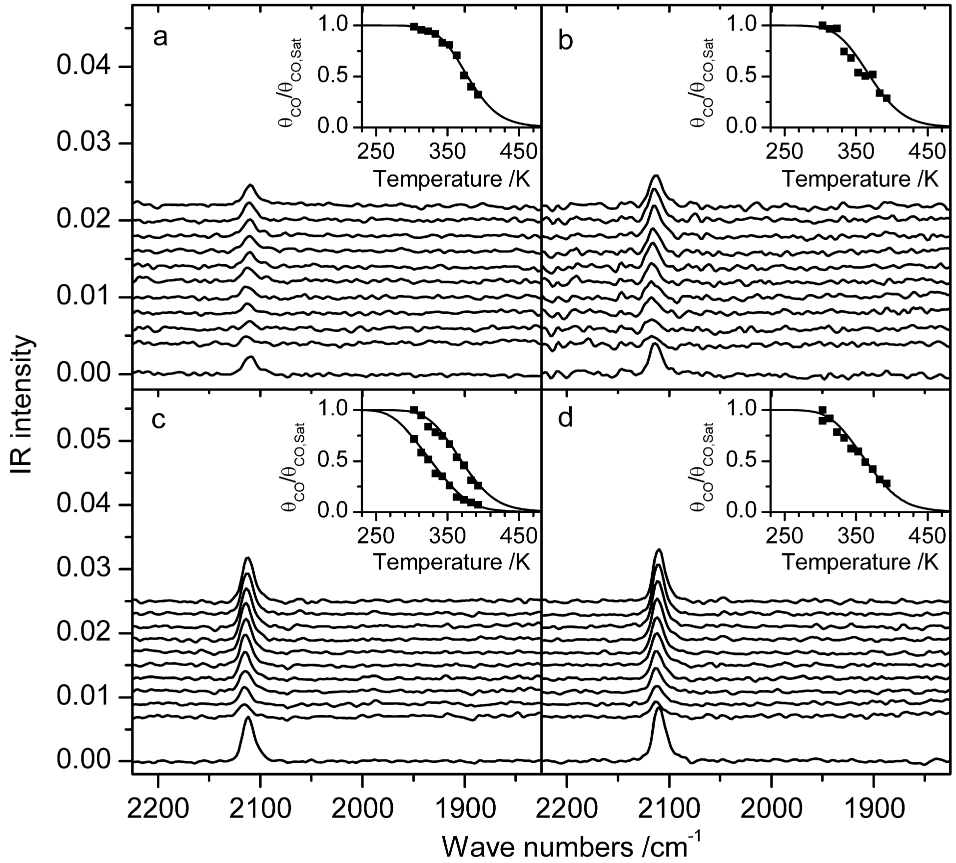

Fig. 3. IR spectra recorded in a 50 mbar CO/$O_2$ (2:1) mixture on Au/$TiO_2$ model catalysts with different nominal Au coverages at varying temperatures: (a) 0.15 ML, (b) 0.24 ML, (c) 0.9 ML, and (d) 1.5 ML. The insets show the evolution of the relative $CO_{ad}$ coverage on the model catalysts with temperature (squares) and the calculated adsorption isobars (full line).

Table 2
CO adsorption energies for adsorption on the Au particles of Au/$TiO_2$ model catalysts in a CO/$O_2$ gas mixture (2:1)

| $\theta_{Au}$ (ML) | $p_{tot}$ (mbar) | $E_0$ (kJ mol$^{-1}$) | $E_1$ (kJ mol$^{-1}$) |
|---|---|---|---|
| 0.15 | 50 | 63 | 53 |
| 0.24 | 50 | 63 | 50 |
| 0.9 | 10 | 63 | 44 |
|  | 50 | 63 | 50 |
| 1.5 | 50 | 63 | 48 |

the presence of oxygen influenced primarily the CO adsorption on model catalysts with smaller Au particles. For model catalysts with approximately 0.2 ML Au (2 nm particle size), the presence of $O_2$ in the gas atmosphere lowered the initial adsorption energy by 10 kJ mol$^{-1}$, whereas the minimum CO adsorption energy increased by around the same value. With increasing Au coverage, the influence of $O_2$ on the CO adsorption energy decreased gradually and eventually almost vanished. These results can be explained by the decreasing adsorption strength of oxygen on the model catalysts with increasing Au particle size. Based on TPD experiments with Au/$TiO_2$ model catalysts, which had been exposed to atomic oxygen, Bondzie et al. [45,46] demonstrated that the adsorption strength of O atoms increased with decreasing Au particle size. In addition, these authors concluded from the Brønsted relation that the dissociative adsorption of $O_2$ molecules similarly should occur more readily on smaller particles. These conclusions were confirmed by later density functional theory calculations by Lopez et al. [47]. In that case, we can expect higher oxygen coverage under steady-state conditions on smaller Au particles, resulting in a more pronounced influence on the adsorption of CO. In contrast, the effects on adsorbed CO are smaller on larger Au particles with a lower tendency for oxygen adsorption.

The slightly lower value of $E_1$ obtained from the 10 mbar isobar compared with that from the 50 mbar measurement (44 vs 50 kJ mol$^{-1}$) may be related to the smaller influence of oxygen due to lower steady-state coverage. As expected, the values of the initial CO adsorption energy, $E_0$, were similar in both cases (63 kJ mol$^{-1}$).

For a molecular-scale understanding of the present results, particularly of the significant changes in CO adsorption characteristics induced by the presence of oxygen, it is important to note that large-scale blocking of CO adsorption sites by adsorbed oxygen is unlikely, because the signal intensity of IR measurements at room temperature using either pure CO or CO/$O_2$ gas mixtures with similar CO partial pressure are almost identical [27]. A rather low steady-state oxygen coverage also can be concluded from the positive reaction order for oxygen under the present reaction conditions, on both dispersed catalysts [16] and model catalysts [44]. However, this does not exclude the possibility that small amounts of strongly adsorbing sites are blocked by oxygen, leaving only sites with lower adsorption energy for CO adsorption. Such competition is indeed plausible, because the undercoordinated Au sites, which are most strongly adsorbing for CO, are also the most favored adsorption sites for oxygen [42,47]. Furthermore, the CO adsorption energy also may be altered by interactions between $CO_{ad}$ and co-adsorbed oxygen, which also lead to a small blue shift of the CO stretching frequency (by $4\ cm^{-1}$) [27]. This shift, which had also been observed for $Au/TiO_2$ powder catalysts [15,16], is assigned to a reduced $\pi$ back-donation from the Au particles to the $CO_{ad}$ in the presence of coadsorbed oxygen. Oxide formation on the Au particles in the $CO/O_2$ gas mixtures can be excluded based on the relatively small blue shift, because on oxidized Au, the peak position of $CO_{ad}$ shifts to $2170\ cm^{-1}$ [48]. This conclusion is also in agreement with the results of recent in situ X-ray absorption spectroscopy (XAS) and X-ray photoemission spectroscopy (XPS) studies on $Au/MeO_x$ powder catalysts and planar model catalysts [49–55]. On $Au/Al_2O_3$ powder catalysts, XAS measurements revealed that the Au atoms maintained their metallic character under reaction conditions ($CO/O_2$ gas mixtures) [49,50], whereas under pure $O_2$, some of the Au atoms were oxidized [50,51]. Similarly, on $Au/TiO_2$ catalysts, in situ XPS measurements with both dispersed powder catalysts and planar model catalysts found no evidence of Au oxidation either under reaction conditions or in pure $O_2$ atmosphere (0.3 mbar) [52,53].

Another possible explanation for the change in the Au adsorption properties for pure CO and $CO/O_2$ gas mixtures, which involves reduction of the substrate surface on interaction with pure CO and electronic modification of the Au particles by interaction with the resulting O vacancies, can be excluded in these measurements, because we kept the CO pressure below the critical value of 20 mbar [20]. The same is true for changes in the Au particle morphology induced by interaction with the respective atmosphere, for example, to a flatter shape on interaction with pure CO. XPS measurements performed after the respective measurements showed no significant change in the Au(4f):Ti(2p) intensity ratio on exposure to 10 mbar CO or to a $CO/O_2$ mixture (2:1, $p_{tot} = 50$ mbar); only for exposure to 50 mbar CO did we find an increase in this ratio.

Therefore, interactions between $CO_{ad}$ and co-adsorbed oxygen, and possibly some blocking of more strongly adsorbing sites by adsorbed oxygen, appear to be the most likely explanation for the oxygen-induced change in CO adsorption energy. Changes in the electronic state or morphology of the Au particles, due to partial reduction of the $TiO_2$ surface by reaction with CO, appear to be unlikely under the present adsorption conditions.

## 4. Conclusion

The energetics of CO adsorption on well-defined planar $Au/TiO_2$ model catalysts with different Au particle sizes under catalytically relevant pressure and temperature conditions were studied by temperature-dependent PM-IRAS measurements. Adsorption energies were determined through a quantitative analysis of the CO absorption intensities during isobaric measurements. Experiments with pure CO showed a decrease in the initial adsorption energy, from 74 to $62\ kJ\,mol^{-1}$ with increasing Au particle size, and a significant decay of the adsorption energy with increasing $CO_{ad}$ coverage, in good agreement with previous results of measurements on $Au/TiO_2$ model catalysts under UHV conditions. Adding $O_2$ to the gas atmosphere led to significant changes in the CO adsorption energies for smaller Au particles; the initial adsorption energy decreased from $74\ kJ\,mol^{-1}$ in pure CO atmosphere to $63\ kJ\,mol^{-1}$ in a $CO/O_2$ mixture at a nominal Au coverage of about 0.2 ML. For larger Au particles, the influence of $O_2$ leveled off, resulting in almost constant initial and minimum adsorption energies of 63 and $48–53\ kJ\,mol^{-1}$, respectively. The small difference between IR intensities in the presence and absence of $O_2$ indicates that significant blocking of CO adsorption sites can be excluded. The effect of oxygen on the CO adsorption energy is attributed to interactions between $CO_{ad}$ and co-adsorbed oxygen and possibly some site blocking, rather than to changes in the electronic state or morphology of the Au particles due to interaction with O vacancies, which can be created by reaction of the $TiO_2$ substrate surface with CO at higher pressure.

## Acknowledgment

This work was supported by the Deutsche Forschungsgemeinschaft (DFG) within the Priority Program (SPP) 1091 (Be 1201/9-5).

## References

[1] M. Haruta, Catal. Today 36 (1997) 153.
[2] G.C. Bond, D.T. Thompson, Catal. Rev.-Sci. Eng. 41 (1999) 319.
[3] M. Haruta, CATTECH 6 (2002) 102.
[4] M. Haruta, M. Daté, Appl. Catal. A 222 (2001) 427.
[5] M.M. Schubert, S. Hackenberg, A.C. van Veen, M. Muhler, V. Plzak, R.J. Behm, J. Catal. 197 (2001) 113.
[6] G. McElhiney, J. Pritchard, Surf. Sci. 60 (1976) 397.
[7] C. Ruggiero, P. Hollins, J. Chem. Soc. Faraday Trans. 92 (1996) 4829.
[8] C. Ruggiero, P. Hollins, Surf. Sci. 377–379 (1997) 583.
[9] J.M. Gottfried, K.J. Schmidt, S.L.M. Schroeder, K. Christmann, Surf. Sci. 536 (2003) 206.
[10] D.C. Meier, V. Bukhtiyarov, D.W. Goodman, J. Phys. Chem. B 107 (2003) 12668.
[11] J. Kim, E. Samano, B.E. Koel, J. Phys. Chem. B 110 (2006) 17512.
[12] M. Mavrikakis, P. Stoltze, J.K. Nørskov, Catal. Lett. 64 (2000) 101.
[13] D. Loffreda, P. Sautet, J. Phys. Chem. B 109 (2005) 9596.
[14] W.-L. Yim, T. Nowitzki, M. Necke, H. Schnars, P. Nickut, J. Biener, M.M. Biener, V. Zielasek, K. Al-Shamery, T. Klüner, M. Bäumer, J. Phys. Chem. C 111 (2007) 445.
[15] M.A. Bollinger, M.A. Vannice, Appl. Catal. B 8 (1996) 417.
[16] B. Schumacher, Y. Denkwitz, V. Plzak, M. Kinne, R.J. Behm, J. Catal. 224 (2004) 449.
[17] F. Boccuzzi, A. Chiorino, M. Manzoli, Surf. Sci. 454–456 (2000) 942.
[18] D.C. Meier, D.W. Goodman, J. Am. Chem. Soc. 126 (2004) 1892.
[19] Z. Zhao, T. Diemant, D. Rosenthal, K. Christmann, J. Bansmann, H. Rauscher, R.J. Behm, Surf. Sci. 600 (2006) 4992.
[20] T. Diemant, Z. Zhao, H. Rauscher, J. Bansmann, R.J. Behm, Top. Catal. 44 (2007) 83.
[21] B. Schumacher, Ph.D. thesis, Ulm University, 2005.
[22] S. Derrouiche, P. Gravejat, D. Bianchi, J. Am. Chem. Soc. 126 (2004) 13010.

[23] S.K. Shaikhutdinov, R. Meyer, M. Naschitzki, M. Bäumer, H.-J. Freund, Catal. Lett. 86 (2003) 211.

[24] C. Lemire, R. Meyer, S.K. Shaikhutdinov, H.-J. Freund, Surf. Sci. 552 (2004) 27.

[25] K.L. Kostov, H. Rauscher, D. Menzel, Surf. Sci. 278 (1992) 62.

[26] D. Bianchi, Curr. Top. Catal. 3 (2002) 161.

[27] T. Diemant, Z. Zhao, H. Rauscher, J. Bansmann, R.J. Behm, Surf. Sci. 601 (2007) 3801.

[28] Z. Zhao, T. Diemant, T. Häring, H. Rauscher, R.J. Behm, Rev. Sci. Instrum. 76 (2005) 123903.

[29] A. Männig, Z. Zhao, D. Rosenthal, K. Christmann, H. Hoster, H. Rauscher, R.J. Behm, Surf. Sci. 576 (2005) 29.

[30] Z. Zhao, Ph.D. thesis, Ulm University, 2006.

[31] D.J.C. Yates, J. Colloid Interface Sci. 29 (1969) 194.

[32] F. Boccuzzi, A. Chiorino, S. Tsubota, M. Haruta, J. Phys. Chem. 100 (1996) 3625.

[33] S. Brunauer, K.S. Love, R.G. Keenan, J. Am. Chem. Soc. 64 (1942) 751.

[34] T. Chafik, O. Dulaurent, J.L. Gass, D. Bianchi, J. Catal. 179 (1998) 503.

[35] O. Dulaurent, K. Chandes, C. Bouly, D. Bianchi, J. Catal. 188 (1999) 237.

[36] O. Dulaurent, K. Chandes, C. Bouly, D. Bianchi, J. Catal. 192 (2000) 273.

[37] O. Dulaurent, K. Chandes, C. Bouly, D. Bianchi, J. Catal. 192 (2000) 263.

[38] O. Dulaurent, X. Courtois, V. Perrichon, D. Bianchi, J. Phys. Chem. B 104 (2000) 6001.

[39] M.L. Kottke, R.G. Greenler, H.G. Tompkins, Surf. Sci. 32 (1972) 231.

[40] M.S. Chen, D.W. Goodman, Science 306 (2004) 252.

[41] M.S. Chen, D.W. Goodman, Catal. Today 111 (2006) 22.

[42] N. Lopez, T.V.W. Janssens, B.S. Clausen, Y. Xu, M. Mavrikakis, T. Bligaard, J.K. Nørskov, J. Catal. 223 (2004) 232.

[43] T.V.W. Janssens, A. Carlsson, A. Puig-Molina, B.S. Clausen, J. Catal. 240 (2006) 108.

[44] T. Diemant, Z. Zhao, J. Bansmann, H. Rauscher, R.J. Behm (2007), in press.

[45] V.A. Bondzie, S.C. Parker, C.T. Campbell, J. Vac. Sci. Technol. A 17 (1999) 1717.

[46] V.A. Bondzie, S.C. Parker, C.T. Campbell, Catal. Lett. 63 (1999) 143.

[47] N. Lopez, J.K. Nørskov, J. Am. Chem. Soc. 124 (2002) 11262.

[48] J.G. Wang, B. Hammer, Top. Catal. 44 (2007) 49.

[49] N. Weiher, A.M. Beesley, N. Tsapatsaris, L. Delannoy, C. Louis, J.A. van Bokhoven, S.L.M. Schroeder, J. Am. Chem. Soc. 129 (2007) 2240.

[50] J.A. van Bokhoven, C. Louis, J.T. Miller, M. Tromp, O.V. Safonova, P. Glatzel, Angew. Chem. 118 (2006) 4767, Angew. Chem. Int. Ed. 45 (2006) 4651.

[51] J.T. Miller, A.J. Kropf, Y. Zha, J.R. Regalbuto, L. Delannoy, C. Louis, E. Bus, J.A. van Bokhoven, J. Catal. 240 (2006) 222.

[52] E.A. Willneff, S. Braun, D. Rosenthal, H. Bluhm, M. Hävecker, E. Kleimenov, A. Knop-Gericke, R. Schlögl, S.L.M. Schroeder, J. Am. Chem. Soc. 128 (2006) 12052.

[53] Y. Denkwitz, S. Kielbassa, B. Schumacher, J. Bansmann, R.J. Behm, P. Schnörch, E. Vass, M. Hävecker, A. Knop-Gericke, R. Schlögl, submitted for publication.

[54] J.C. Fierro-Gonzalez, J. Guzman, B.C. Gates, Top. Catal. 44 (2007) 103.

[55] J.D. Henao, T. Caputo, J.H. Yang, M.C. Kung, H.H. Kung, J. Phys. Chem. B 110 (2006) 8689.